frontiers | Frontiers in Earth Science

TYPE Original Research
PUBLISHED 06 January 2023
DOI 10.3389/feart.2022.1047535

OPEN ACCESS

EDITED BY
Hu Li,
Southwest Petroleum University, China

REVIEWED BY
Guodong Yang,
Wuhan University of Science and Technology, China
Xinghua Yang,
Shanxi Normal University, China

*CORRESPONDENCE
Shaocong Ji,
jishaocong@mail.cgs.gov.cn

SPECIALTY SECTION
This article was submitted to Structural Geology and Tectonics, a section of the journal Frontiers in Earth Science

RECEIVED 18 September 2022
ACCEPTED 24 October 2022
PUBLISHED 06 January 2023

CITATION
Zhang Q, Liang B, Ji S and Li J (2023), Isotopic characteristics of carbon and oxygen within ordovician carbonate paleokarst in the tazhong region and their paleoenvironmental significance. *Front. Earth Sci.* 10:1047535. doi: 10.3389/feart.2022.1047535

Isotopic characteristics of carbon and oxygen within ordovician carbonate paleokarst in the tazhong region and their paleoenvironmental significance

Qingyu Zhang[1,2], Bin Liang[1,2], Shaocong Ji[1,2]* and Jingrui Li[1,2]

[1]Institute of Karst Geology, Chinese Academy of Geological Sciences Karst Dynamics Laboratory, Ministry of Natural Resources, Guilin, China, [2]International Research Center on Karst Under the Auspices of UNESCO, National Center for International Research on Karst Dynamic System and Global Change, Guilin, China

The Tazhong region is a key area for oil and gas exploration and development within the Tarim basin. In this region, development of Ordovician carbonate paleokarsts has been found to be extremely heterogeneous. To investigate the developmental stages of these Ordovician carbonate karsts and their corresponding paleoenvironmental conditions, oxygen and carbon isotopic characteristics of calcite paleokarst fissure fillings were examined in conjunction with rock-structure analyses. Results show that $\delta^{18}O$ (PDB) values tend towards negative values in general, ranging from −3.97% to −12.7% (average value −7.64%), which is indicative of the presence of paleokarstification *via* dissolution by atmospheric freshwater. Values of $\delta^{13}C$ (PDB) span a relatively large range, from 2.48% to −2.13% (average value of 0.23%). This shows that the paleokarst in this area has gone through two stages of supergene and burial diagenesis, and the process of paleokarst is complex. The paleotemperature at which the karst fissure-filling deposits were formed ranged from 6.5 to 47.1°C (average value of 21.8°C), and the salinity of the medium has Z values from 117.48 to 130.24 (average value of 123.94). Four different paleokarsification settings were thus revealed: a marine depositional environment, an atmospheric freshwater karst-filling environment, a shallow-burial paleokarsification environment and a deep-burial high-temperature environment. It has thus been shown that the karst pores, fissures and caves formed by paleokarstification over multiple stages are the main reservoir spaces in this region. This study will serves as a basis for karst reservoir predictions, and exploration and development in this region.

KEYWORDS

carbon-oxygen isotopes, paleokarsts, paleoenvironments, carbonates, ordovician, tarim basin

Introduction

Tarim Basin is the largest oil and gas sedimentary basin in China (Wu et al., 2012), and karst reservoirs, such as the pores, fissures and caves that are formed due to paleokarstification, are important reservoir spaces in carbonate rocks (Wang and Al-Aasm 2002; Chen et al., 2007; Zhang et al., 2011). Deep-burial karst reservoirs are an important type of reservoir in marine carbonate oil and gas fields. These have generally undergone long periods of geological and environmentally driven changes, including repeated dissolution and filling caused by various factors and fluids. These reservoirs are characteristically very deeply buried, tectonically complex and highly heterogeneous (Li et al., 1996; Zhu et al., 2005), thus causing immense difficulties in predicting the location and character of deeply buried carbonate paleokarst reservoirs (Li, 2022a; Li et al., 2019; Li et al., 2022; Li et al., 2022b; Zhang et al., 2022a; Zhang et al., 2022b; Zhang et al., 2022c; Zhang et al., 2022d).

The carbon and oxygen isotopic compositions of marine carbonates from different geological periods are directly affected by the diagenetic fluids that were generated in each developmental period, and they can serve as an important background value for studies on diagenesis (Arthur et al., 1988; Huang et al., 2014). Under different climatic conditions, carbon and oxygen isotopes will have correspondingly different enrichment characteristics, which are stable over time and have excellent regional comparability (Taylor 1968; Li and Wan 1999; Valley and Cole 2001). Therefore, the carbon and oxygen isotope compositions of carbonate karst fissure fillings are some of the most important tracers in paleoclimatic studies and paleogeological environment reconstructions, and are also highly significant for studies on the development of paleokarsts and karst reservoirs (Tian and Zheng 1995).

In 1948, Nobel Prize winner H.C. Urey suggested that $\delta^{18}O$ values may be used to examine paleoocean temperature (Urey, 1948; Kuypers et al., 1999). In Epstein and Mayeda, 1953 further realized Urey's theory; they established the basic principles for using $\delta^{18}O$ values to calculate paleosalinity levels and determined that the $\delta^{18}O$ value increased with increases in salinity. For a long time, experts and scholars have made great progress in studying the sedimentary environment and diagenesis of carbonate rocks in the Tarim Basin by using the stable carbon and oxygen isotopic composition of carbonate rocks (Zhang et al., 2015; Zhang et al., 2016a; Zhang et al., 2016b; Zhong et al., 2012; Gao et al., 2011; Zhao et al., 2012). Furthermore, much research has been performed using the carbon and oxygen isotope compositions of karst cave-filling stalagmites and stalactites to reconstruct paleoclimates and paleoenvironments since the Permian period (Liu et al., 1997; Liu et al., 2004; Zhang et al., 2015; Huang et al., 2016).

The Ordovician carbonate karst cave systems of the Tazhong region in the Tarim basin are buried in the range of 5550–6480 m beneath the surface, and the development of karst pores, fissures, caves and large-scale underground river systems in this region is highly heterogeneous. With continuous improvements in oil and gas exploration and development technologies in the Tazhong region, ancient karst reservoirs have become the most important type of reservoir in carbonate formations. However, distinguishing the various developmental stages of karst remains a major issue, which restricts the geological modeling of karst reservoirs formed under different phases of karst development, and presents problems for the prediction of favorable regions in effective karst reservoirs.

The distribution patterns and controlling factors of karst reservoirs have previously been studied in the Tazhong region (Han et al., 2012; Liu et al., 2013). Luo et al. (2011) have performed a thorough study of how reservoirs are altered by the developmental characteristics of fissures; additional studies have addressed reservoir traps, geological structure and diagenesis (Yang et al., 2012). However, studies of the carbon and oxygen isotope characteristics of Ordovician carbonate karst fillings in this region are relatively superficial, and the results of existing studies are rather controversial (Shen 2006). Thus, contemporary understanding of the region's patterns of change is relatively weak. In this work, drilled cores of karst fillings from various depths were systematically obtained, and multivariate statistical methods were applied to investigate the geochemical carbon and oxygen isotope characteristics of karst fissure fillings, to evaluate the developmental stages of the paleokarsts in this region, and to assess the environment of its fillings. This work will provide new geochemical information that will improve scientific understanding of the developmental patterns of karst reservoirs.

Study area and methodology

Geographical setting

The Tazhong region is located in a low rise in the middle of the central uplift of the Tarim basin, and it is a large, mostly intact anticline composed of multiple secondary structural belts (Han et al., 2012; Sun et al., 2012). The region can be further divided into 3 tectonic elements: the Tazhong No. 1 Fault, the Tazhong North Slope, and the Central Fault Belt (Figure 1). The Tazhong No. 1 Fault controls the basic structure of the Tazhong Uplift. During the Early-Middle Ordovician, the Tazhong No. 1 Fault caused severe erosion within the Tazhong Uplift, which formed the weathering crust at the top of the Yingshan Formation of the Lower Ordovician. During this period, the Yijianfang Formation of the Middle Ordovician and Tumuxiuke Formation of the Upper Ordovician suffered erosion or loss, with remnants remaining only in certain locations.

The Ordovician layers of the Tazhong region are mainly composed of the Lower Ordovician Penglaiba (O_1p) and Yingshan (O_1y) Formations, and the Upper Ordovician

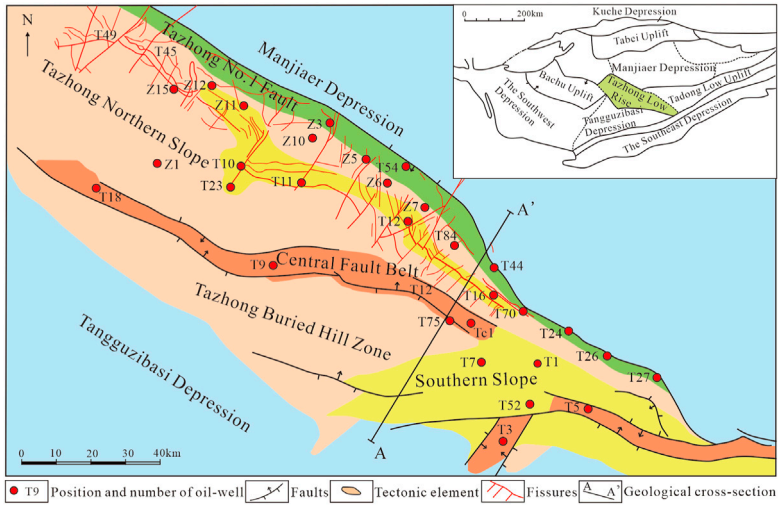

FIGURE 1
Geological map of tectonics and distribution of sampled wells within the Tazhong region of the Tarim basin.

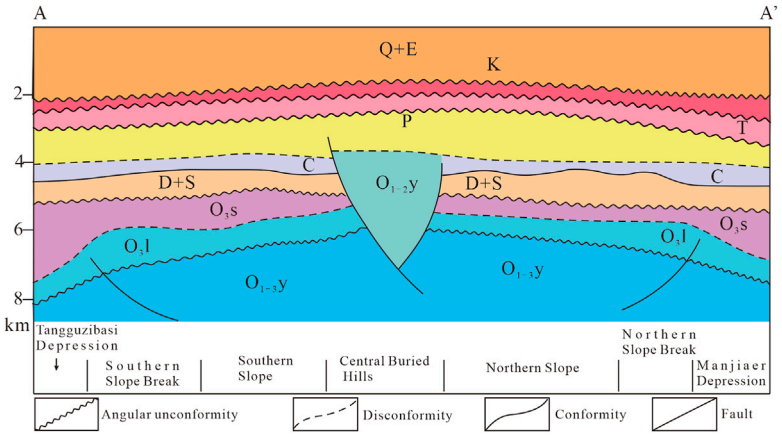

FIGURE 2
Schematic diagram of geological cross-section of the Tazhong Uplift in the southwest-to-northeast direction.

Lianglitag (O_2l) and Sangtamu (O_3s) Formations. The Upper Ordovician layer is not fully in contact with the overlying Silurian layer and the underlying Lower Ordovician layer. As compared to the stratigraphy of the Tabei region (Liu et al., 2013; Lu 2015), the Tazhong region is missing the layers corresponding to the Middle Ordovician Yijiangfang and Upper Ordovician Tumuxiuke Formations (Figure 2). The Yingshan Formation in the Tazhong region is dominated by high-energy sandy deposits with multiperiodic developments in the vertical direction that overlap with each other. The formation is relatively large in scale, and stretches from the northeast to the southeast, with a linear shape and belt-like distribution. The large, thick sets of shoal bodies that have developed over time are the basis for karst developments in the Yingshan Formation. The depositional discontinuity in this region provides favorable conditions for the development of karst in the carbonates of the Lower Ordovician Yingshan Formation. Exploration works have shown that the Lower Ordovician Yingshan Formation has large fractured karst reservoirs, and is thus a very important oil and gas producing stratum within carbonates in this region.

The Yingshan Formation in Tazhong can be divided into four segments from the bottom to the top. The lithology of the fourth segment ($O_{1\text{-}2}y^4$) mainly comprises sandy dolarenite,

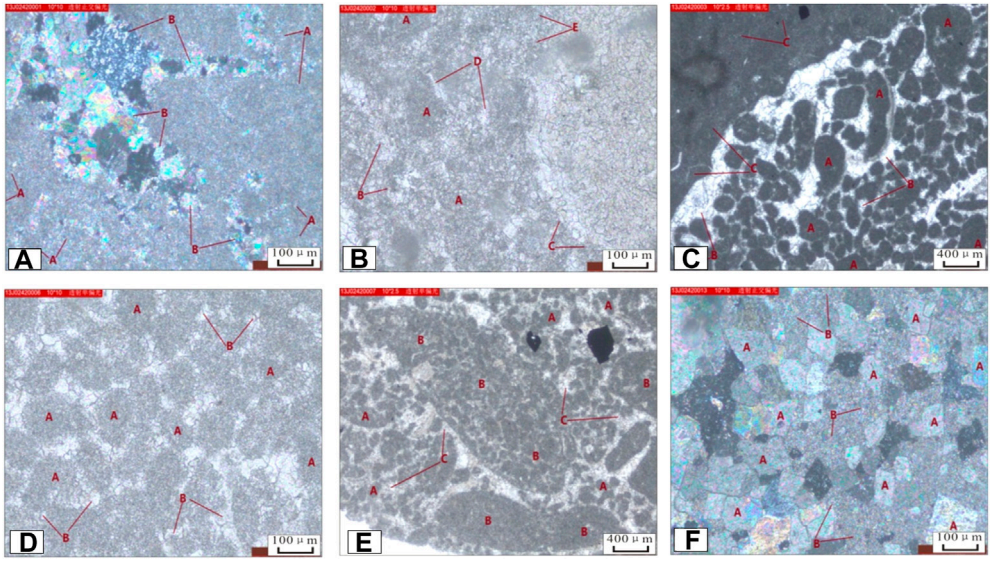

FIGURE 3
Petrological characteristics of carbonates from the Ordovician Yingshan Formation. **(A)**: T43-1 depth of 5280 m, O1-2y, microcrystalline limestone, orthogonally-polarized transmission 10*10. A: microcrystalline calcite, B: recrystallized calcite; **(B)**: T43-1, depth of 5285 m, O1-2y, fine-grained calcarenite, single-polarized transmission, 10**10. A: sand chip, B: powdered calcite, C: microcrystalline calcite, D: sparry calcite, E: powdery crumbs; **(C)**: 542, depth of 5289 m, O1-2y, micritic sparry calcarenite, single-polarized transmission, 10*2.5. A: sand chip, B: sparry calcite, C: argillaceous calcite ; **(D)**: T42-1, depth of 5273 m, O1-2y, sparry calcarenite, single-polarized transmission, 10*10. A: sand chip, B: sparry calcite; **(E)**: T44, depth of 5269 m, O1-2y, sparry calcirudite, single-polarized transmission, 10*2.5. A: sand chip, B: gravelly debris, C: sparry calcite; **(F)**: T8-5, depth of 6175 m, O1-2y, fine-grained dolomite with intense dolomitization, orthogonally-polarized transmission, 10*10. A: dolomite, B: calcite.

dolomitic micritic limestone and finely-crystalline dolomite; the lithology of the third segment (O_1-$2y^3$) mainly comprises dolomitic micritic limestone; the lithology of the second segment ($O_{1\text{-}2}y^2$) is mainly interbedded calcarenite and dolomitic micritic limestone; the first segment can be divided into an upper sub-segment ($O_{1-2}y^{1\text{upper}}$) and lower sub-segment ($O_{1-2}y^{1\text{lower}}$), with the lower sub-segment being composed of a thick layer of sparry calcarenite, while the upper sub-segment is mainly composed of micritic calcarenite sandwiching a thin layer of micritic limestone (Figure 3). As a result, the Yingshan Formation is being eroded layer by layer from the north towards the south, and the exposed strata are gradually declining. This erosion occurs in parallel with the direction of the Tazhong No. 1 Fault in a strip-like distribution. Around the Tazhong No. 1 Fault, the upper and lower sub-segments of the first Yingshan segment are being exposed sequentially. In the south, the second ($O_{1-2y}{}^2$) and third ($O_{1-2y}{}^3$) Yingshan segments are being exposed around the Tazhong No. 1 Fault.

A: T43-1 depth of 5280 m, $O_{1\text{-}2}y$, microcrystalline limestone, orthogonally-polarized transmission 10*10. A: microcrystalline calcite, B: recrystallized calcite; b: T43-1, depth of 5285 m, $O_{1\text{-}2}y$, fine-grained calcarenite, single-polarized transmission, 10*10. A: sand chip, B: powdered calcite, C: microcrystalline calcite, D: sparry calcite, E: powdery crumbs; c: 542, depth of 5289 m, $O_{1\text{-}2}y$, micritic sparry calcarenite, single-polarized transmission, 10*2.5. A: sand chip, B: sparry calcite, C: argillaceous calcite; d: T42-1, depth of 5273 m, $O_{1\text{-}2}y$, sparry calcarenite, single-polarized transmission, 10*10. A: sand chip, B: sparry calcite; e: T44, depth of 5269 m, $O_{1\text{-}2}y$, sparry calcirudite, single-polarized transmission, 10*2.5. A: sand chip, B: gravelly debris, C: sparry calcite; f: T8-5, depth of 6,175 m, $O_{1\text{-}2}y$, fine-grained dolomite with intense dolomitization, orthogonally-polarized transmission, 10*10. A: dolomite, B: calcite.

Samples and experiment

The experimental samples were mainly obtained from 25 Ordovician cores of paleokarst fissure fillings drilled from various depths within the Tazhong region of the Tarim basin (Figure 1), with a total of 49 samples. All samples were obtained in a range of 1.25–480 m below the top of the Ordovician strata, and the depths at which the samples were obtained, from the surface, ranged from 5553.5 m to 6,472.5 m. Three of the obtained samples were limestone samples of the Yingshan Formation, while the remaining 46 samples were karst fissure fillings (4 of which were grey-green calcite mudstone fillings, while 42 were samples of calcite fillings) (Table 1). These obtained samples are representative of the overall characteristics of karstification in the Ordovician carbonates of the Tazhong region.

TABLE 1 Carbon and oxygen isotopic characteristics of Ordovician carbonate karst fissure fillings from the Tazhong region.

Sampled well	Well depth of sample (m)	Stratum	Type of paleokarst fracture/ cavity	Lithological characteristics of filling	Isotopic characteristics		$\delta^{18}O_{Correction}$	Paleotemperature	Paleosalinity
					$\delta^{13}C$(PDB)	$\delta^{18}O$(PDB)			
					‰	‰		(°C)	Z value
T49	5553.5	$O_{1\text{-}2}y$	Dissolved cavity	Calcite	−0.4	−10.76	−4.32	36.3	121.12
T201-1H	5876.4	$O_{1\text{-}2}y$	Dissolved cavity	Calcite	−0.13	−6.29	0.15	15.4	123.90
T201-1H	5898.5	$O_{1\text{-}2}y$	Dissolved cavity	Calcite	0.25	−7.89	−1.45	22.3	123.88
T452	5897.3	$O_{1\text{-}2}y$	Dissolved cavity	Calcite	0.6	−5.76	0.68	13.2	125.66
T452	5913.7	$O_{1\text{-}2}y$	Dissolved cavity	Calcite	−0.53	−8.28	−1.84	24.0	122.09
T452	6243.2	$O_{1\text{-}2}y$	Dissolved fracture	Calcite	0.58	−8.6	−2.16	25.5	124.21
Z3	5699.3	$O_{1\text{-}2}y$	Dissolved fracture	Calcite	0.76	−11.83	−5.39	42.1	122.97
Z9	6162.6	$O_{1\text{-}2}y$	Dissolved fracture	Calcite	0.15	−12.41	−5.97	45.3	121.43
Z171	5973.5	$O_{1\text{-}2}y$	Dissolved fracture	Calcite	0.09	−9.11	−2.67	28.0	122.95
Z171	5999.5	$O_{1\text{-}2}y$	Dissolved fracture	Calcite	−0.23	−8.79	−2.35	26.4	122.45
Z442H	6276.1	$O_{1\text{-}2}y$	Dissolved fracture	Calcite	−1.76	−11.11	−4.67	38.2	118.16
Z442H	6302.5	$O_{1\text{-}2}y$	Dissolved fracture	Calcite	−1.68	−9.21	−2.77	28.5	119.27
Z105H	6352.3	$O_{1\text{-}2}y$	Bedrock	Limestone	0.33	−5.21	1.23	11.1	125.38
Z43-1	5825.6	$O_{1\text{-}2}y$	Bedrock	Limestone	0.02	−5.94	0.5	13.9	124.38
Z43-1	5859.6	$O_{1\text{-}2}y$	Bedrock	Limestone	−0.38	−7.16	−0.72	19.0	122.96
Z43-1	5967.3	$O_{1\text{-}2}y$	Dissolved Cavity	Calcium mudstone	0.8	−5.76	0.68	13.2	126.07
Z43-1	6055.8	$O_{1\text{-}2}y$	Dissolved Cavity	Calcium mudstone	0.99	−5.76	0.68	13.2	126.46
Z43-1	6132.8	$O_{1\text{-}2}y$	Dissolved Cavity	Calcium mudstone	1.04	−6.7	−0.26	17.1	126.09
Z43-1	6276.9	$O_{1\text{-}2}y$	Dissolved Cavity	Calcium mudstone	0.66	−6.48	−0.04	16.1	125.42
T12	6324.3	$O_{1\text{-}2}y$	Dissolved Fracture	Calcite	−1.79	−8.39	−1.95	24.6	119.46
T12	6358.7	$O_{1\text{-}2}y$	Dissolved Fracture	Calcite	−1.43	−8.33	−1.89	24.3	120.22
T12	6472.5	$O_{1\text{-}2}y$	Dissolved Fracture	Calcite	0.87	−9.08	−2.64	27.8	124.56
T35	6123.7	$O_{1\text{-}2}y$	Dissolved Fracture	Calcite	2.4	−3.97	2.47	6.5	130.24
T35	6153.4	$O_{1\text{-}2}y$	Dissolved Fracture	Calcite	2.38	−5.12	1.32	10.7	129.62
T35	6198.6	$O_{1\text{-}2}y$	Dissolved Fracture	Calcite	2.11	−4.45	1.99	8.3	129.41
T63	5783.2	$O_{1\text{-}2}y$		Calcite	1.83	−5.52	0.92	12.3	128.30

(Continued on following page)

10.3389/feart.2022.1047535

TABLE 1 (*Continued*) Carbon and oxygen isotopic characteristics of Ordovician carbonate karst fissure fillings from the Tazhong region.

Sampled well	Well depth of sample (m)	Stratum	Type of paleokarst fracture/ cavity	Lithological characteristics of filling	Isotopic characteristics		$\delta^{18}O_{Correction}$	Paleotemperature	Paleosalinity
					$\delta^{13}C$(PDB)	$\delta^{18}O$(PDB)			
					‰	‰		(°C)	Z value
			Dissolved Fracture						
T63	5976.3	$O_{1\text{-}2}y$	Dissolved Fracture	Calcite	0.77	−8.15	−1.71	23.4	124.82
T83	6218.5	$O_{1\text{-}2}y$	Dissolved Fracture	Calcite	1.01	−5.09	1.35	10.6	126.83
T83	6242.5	$O_{1\text{-}2}y$	Dissolved Fracture	Calcite	1.16	−5.52	0.92	12.3	126.93
T84	6012.7	$O_{1\text{-}2}y$	Dissolved Fracture	Calcite	0.57	−10.71	−4.27	36.0	123.13
T84	6033.2	$O_{1\text{-}2}y$	Dissolved Fracture	Calcite	0.34	−5.86	0.58	13.6	125.08
T84	6051.1	$O_{1\text{-}2}y$	Dissolved Fracture	Calcite	−0.51	−8.87	−2.43	26.8	121.84
T162	5568.4	$O_{1\text{-}2}y$	Dissolved Fracture	Calcite	−2.13	−10.95	−4.51	37.3	117.48
T201-1H	5595.5	$O_{1\text{-}2}y$	Dissolved Fracture	Calcite	0.24	−6.8	−0.36	17.5	124.41
T201-1H	5742.6	$O_{1\text{-}2}y$	Dissolved Fracture	Calcite	−1	−12.7	-6.26	47.0	118.93
Z29	5553.5	$O_{1\text{-}2}y$	Dissolved Fracture	Calcite	2.48	−5.42	1.02	11.9	129.68
Z32	6311.2	$O_{1\text{-}2}y$	Dissolved Fracture	Calcite	−1.3	−9.51	−3.07	29.9	119.90
Z41	5818.9	$O_{1\text{-}2}y$	Dissolved Fracture	Calcite	−1.21	−4.26	2.18	7.6	122.70
Z41	5845.3	$O_{1\text{-}2}y$	Dissolved Fracture	Calcite	−1.57	−7.61	−1.17	21.0	120.29
Z41	5866.9	$O_{1\text{-}2}y$	Dissolved Fracture	Calcite	−2.63	−8.44	−2	24.8	117.71
Z43-1	6012.7	$O_{1\text{-}2}y$	Dissolved Fracture	Calcite	−0.17	−9.77	−3.33	31.2	122.09
Z49	5990.5	$O_{1\text{-}2}y$	Dissolved Cavity	Calcite	1.67	−8.26	−1.82	24.0	126.61
Z49	6018.4	$O_{1\text{-}2}y$	Dissolved Cavity	Calcite	2.31	−7.08	-0.64	18.7	128.51

(Continued on following page)

10.3389/feart.2022.1047535

TABLE 1 (*Continued*) Carbon and oxygen isotopic characteristics of Ordovician carbonate karst fissure fillings from the Tazhong region.

Sampled well	Well depth of sample (m)	Stratum	Type of paleokarst fracture/ cavity	Lithological characteristics of filling	Isotopic characteristics		$\delta^{18}O_{Correction}$	Paleotemperature	Paleosalinity
					$\delta^{13}C$(PDB)	$\delta^{18}O$(PDB)			
					‰	‰		(°C)	Z value
Z49	6037.8	$O_{1-2}y$	Dissolved Cavity	Calcite	2.03	−4.74	1.7	9.3	129.10
Z49	6051.2	$O_{1-2}y$	Dissolved Fracture	Calcite	2.22	−6.08	0.36	14.5	128.82
Z51	5734.6	$O_{1-2}y$	Dissolved Fracture	Calcite	−0.23	−11.05	−4.61	37.8	121.33
Z106	5835.8	$O_{1-2}y$	Dissolved Fracture	Calcite	−0.57	−5.08	1.36	10.6	123.60
Z166H	5973.3	$O_{1-2}y$	Dissolved Fracture	Calcite	0.47	−4.64	1.8	8.9	125.95
Z171	6217.4	$O_{1-2}y$	Dissolved Fracture	Calcite	−1.08	−9.9	−3.46	31.9	120.16

After the samples were observed as slices, fresh sections were then ground to 200-mesh, and an on-line analysis of the carbon and oxygen isotope values was performed using a combination of the Gasbench II and MAT253 system. The accuracy of the analysis was calibrated using the GBW04405, GBW04406, GBW04416 and GBW04417 Chinese national standards, with the NBS18 standard being used for monitoring measurements. The standard deviations of the $\delta^{13}C$ and $\delta^{18}O$ values were found to be 0.005% and 0.07%, respectively. The test results were reported in the PDB standard, and the temperature and humidity at which the tests were performed at were 25°C and 60%, respectively. The serial number of the test is QC-2-030-2013. The testing of the samples was performed at the Karst Geology Resources and Environment Test Center of the Ministry of Land and Resources.

Results and analysis

Geochemical characteristics of carbon and oxygen isotope values

The ^{13}C and ^{18}O enrichment levels of marine carbonates are mainly affected by factors such as sea level rises and falls, organic carbon sources, burial rates, and the redox conditions within the diagenetic environment of the sediment (Zheng and Chen, 2000). Hence, changes of diagenetic environment and properties of diagenetic fluid in sediments will change the resulting carbon and oxygen isotopic compositions of the carbonates. The results of the analysis of carbon and oxygen isotopes in the 49 limestone and calcite Ordovician carbonate filling samples from the Tazhong region (42 calcite samples, 4 calcite mudstone samples and 3 limestone samples) are shown in Table 1.

Many test results based on the PDB standard have shown that most modern inorganic marine carbonates have $\delta^{13}C$ and $\delta^{18}O$ values that approach 0% (Gu 2000; Liu et al., 2004). Based on the test results of the samples (Table 1), the Ordovician carbonate karst fissure fillings from the Tazhong region have $\delta^{13}C$ and $\delta^{18}O$ values that are clearly distinct from modern values, and they also have a high level of variability. The $\delta^{13}C$ (PDB) values ranged from 2.48% to −2.13%, and had an average value of 0.23%; the $\delta^{18}O$ values ranged from −3.97% to −12.7%, with an average value of −7.64%.

Compared to previous examinations of older carbonates, this study's results are distinctly different from those of Gu (2000), Liu et al. (2008) and Gao et al. (2011). Gu (2000) found an average $\delta^{18}O$ isotope value of −4% to −5% for Devonian to Cambrian marine carbonates. Liu et al. (2008) found that the $\delta^{13}C$ values of microcrystalline limestone from the Tahe oilfields were distributed between −1.697% and 0.921%, with an average value of −0.45%; the corresponding $\delta^{18}O$ values were distributed between −8.64% and −4.153%. Gao et al. (2011) found that the marine carbonates in the outcrop zone of Tabei to have $\delta^{13}C$ and $\delta^{18}O$ values ranging between −5.0% and 5.0% and −6.0%

to −4.0%, respectively. These results uniformly display a characteristically high level of ^{18}O depletion.

Liu et al. (2004) found that the calcite fillings of Ordovician carbonate karst fissures from Lunguxi had $\delta^{13}C$ values of −0.70% to −6.50%, with an average value of −1.76%, and $\delta^{18}O$ values of −3.75%–17.10%, with an average value of −9.42%. This is similar to the carbon and oxygen isotopic characteristics of calcite Ordovician karst fissure fillings from the Tahe oilfields (average $\delta^{13}C$ and $\delta^{18}O$ values of −0.807% and −9.14% from 21 data points; Liu et al., 2008).

The Lungudong (average $\delta^{13}C$: −1.40%, average $\delta^{18}O$: −10.74%, 25 data points; Zhang et al., 2015) and Lunguxi [$\delta^{13}C$ (PDB): 6.03% to −8.69%, average $\delta^{13}C$: −1.40%; $\delta^{18}O$: −5.78%–17.28%, average $\delta^{18}O$: −10.74%; Zhang et al., 2016a] regions, as well as the Halahatang region ($\delta^{13}C$ (PDB): 2.12% to −4.09%, average $\delta^{13}C$: −0.65%; $\delta^{18}O$: −4.14% to −15.71%, average $\delta^{18}O$: −9.95%) are not very different from each other, with only a few data points drifting towards extreme values (Zhang et al., 2016b).

The $\delta^{13}C$ and $\delta^{18}O$ distributions in calcite and calcite mudstone samples obtained from reservoir spaces such as dissolved cavities and fractures within the Tazhong region have significant variability. Nonetheless, the $\delta^{18}O$ values are distinctly negative-biased, with an average value of -7.64%; the $\delta^{13}C$ values tend towards both negative and positive extremes, which reflects on a paleogeological environment in which paleokarstification occurred *via* shallow to deep burial karstification, followed by alterations and filling through dissolution in later periods. The distribution of $\delta^{13}C$ values from 2.48% to −2.13% with nearly equal positive and negative distributions provides further proof of the complexity of paleokarstification processes in this region.

Relationship between paleosalinity levels and carbon/oxygen isotopic ratios

The analysis of stable carbon and oxygen isotopic ratios is a frequently used procedure in paleoenvironmental studies, as these ratios reflect the sedimentary environment and typically change across stratigraphic boundaries (Guo et al., 2010). In seawater, the $\delta^{18}O$ value increases as salinity increases (Wang et al., 2014), since ^{16}O is preferentially evaporated and transformed into atmospheric precipitation; the remaining seawater, which is now higher in salinity, becomes enriched in ^{18}O. However, as $\delta^{18}O$ levels are more strongly affected by karstification, they are less accurate as a measure of primitive sedimentary environments (Wang et al., 2014). Zhang (1985) analyzed the isotopic compositions of Cambrian and Ordovician carbonate samples obtained from various regions of China, and found that during karstification, the isotopic exchange reaction between ^{13}C and ^{12}C is significantly weaker than that between ^{18}O and ^{16}O. Hence, the isotopic composition of carbon can reflect changes in primitive sedimentary environments.

Keith and Weber (1964) derived the following empirical equation using $\delta^{13}C$ and $\delta^{18}O$ values in limestone to produce a criterion for discriminating between marine and non-marine carbonates:

$$Z = 2.048 \times (\delta^{13}C + 50) + 0.498 \times (\delta^{18}O + 50) \quad (1)$$

The $\delta^{13}C$ and $\delta^{18}O$ values in the formula are both in the PDB standard. Marine carbonates have $Z > 120$, while freshwater carbonates have $Z < 120$. When $Z = 120$, the environment of the carbonate is then of the uncertain type. This conclusion has been confirmed by many subsequent research results (Zhong et al., 2012). Table 1 shows that the $\delta^{13}C$ values of the 49 tested samples are distributed within the range of −2.63%–2.48%, while the distribution range of their Z values is 117.48–130.24. Except for 7 samples that had a distribution between 117.48–119.9, the remaining 42 samples had Z values larger than 120, within a distribution range of 120.16–130.24. This signifies that development and filling processes of the karst fracture/cavity systems in the Tazhong region have been modified by a multitude of superimposed karstification processes, including freshwater karstification of the paleoweathering crust, karstification by a mix of seawater and freshwater, as well as burial karstification.

Analysis of the correlations between $\delta^{13}C$ and $\delta^{18}O$ with Z (Figures 4A,B) show that the $\delta^{13}C$ values in this region correlate very well with Z, with a correlation coefficient of 0.9560, but $\delta^{18}O$ correlates poorly with Z, and has a correlation coefficient of only 0.7414. This indicates that isotopic fractionation in carbonates is mainly controlled by the redox conditions of the environment, and $\delta^{13}C$ and $\delta^{18}O$ are both affected by medium salinity, with $\delta^{13}C$ particularly showing a significant level of correlation with the salinity of the medium (Keith and Weber 1964; Zhang 1985; Wang et al., 2014).

The relationship between oxygen isotopic ratios and paleotemperatures

The primary factor that determines oxygen-isotope ratios in carbonate depositional environments is temperature, so changes in the oxygen-isotope content reflect changes in paleotemperature in the diagenetic environment (Scholle and Arthur 1980; Huang et al., 2014). Lower $\delta^{18}O_{PDB}$ values reflect higher paleotemperatures, and higher $\delta^{18}O_{PDB}$ values conversely reflect a lower paleotemperature.

A calibration for the "periodic effect" was performed based on the correlation between $\delta^{18}O$ values and geological period given by Keith and Weber (1964), with the average $\delta^{18}O$ value of karst fillings in the Tazhong region being −7.64%. The average $\delta^{18}O$ value of marine limestones from the Paleozoic era is approximately −1.2%, which differs by −6.44% from the average found in this study. An average

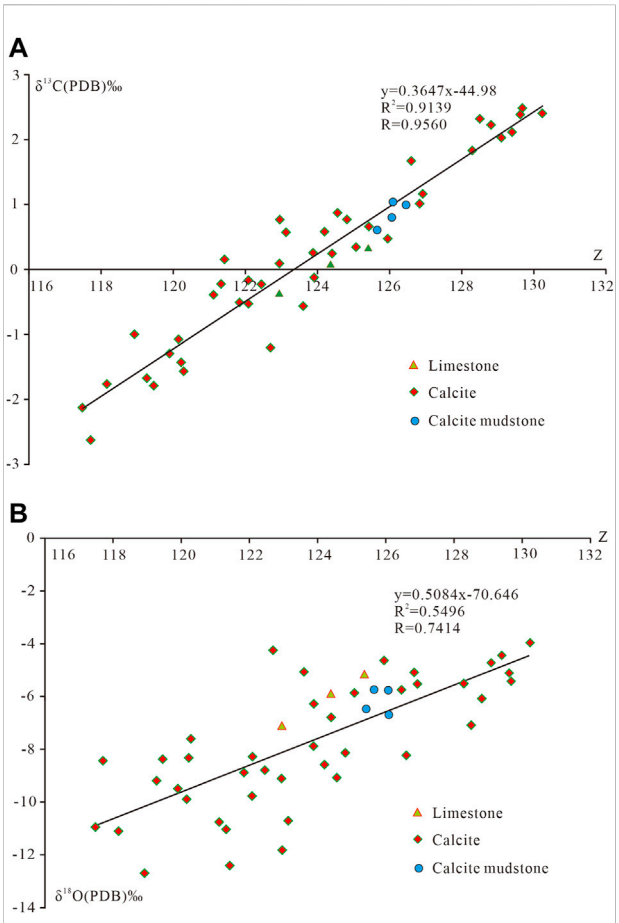

FIGURE 4
(A) The δ13C-Z correlation of Ordovician paleokarst fissure fillings from the Tazhong region. **(B)** The δ18O-Z correlation of Ordovician paleokarst fissure fillings from the Tazhong region.

$\triangle\delta^{18}O$=6.44‰ was then used as the calibration value for the "periodic effect" (Shao 1994).

The paleotemperature was calculated using the formula derived by Craig (1961) based on the relationship between the oxygen isotopic ratio and paleotemperature.

$$T(℃) = 16.9 - 4.2 \times (\delta O_c - \delta O_w) + 0.13 \times (\delta O_c - \delta O_w)^2 \quad (2)$$

In this formula, the equivalence $\delta O_c - \delta O_w = (\delta^{18}OCaCO3 - \delta^{18}OH2O) + 0.22$ was used, since the $\delta^{18}O$ value of $CaCO_3$ obtained in the lab is in the PDB standard, while the $\delta^{18}O$ of water is in the SMOW (Standard Mean Ocean Water) standard; the calculated $\delta^{18}OCaCO3$ thus needed to be calibrated in temperature calculations using Eq. 2. As the $\delta^{18}O$ value of the Ordovician ocean remains unknown for now, it was temporarily assumed to be the same as that of modern oceans; i.e., $\delta^{18}OH2O = 0$ (SMOW standard) (Shao 1994).

Hence, in this study's calculations on the paleotemperatures of karst fillings and the carbonate matrix from the Tazhong region, the overall equation for calculating the paleotemperature of karst filling samples is:

$$T(℃) = 16.9 - 4.2 \times \left(\delta^{18}O_{CaCO_{3correction}} + 0.22\right) + 0.13 \times \left(\delta^{18}O_{CaCO_{3correction}} + 0.22\right)^2 \quad (3)$$

These calculations have shown that the Formation paleotemperatures of Ordovician carbonate karst fillings from the Tazhong region ranged from 6.5°C to 47.1°C, with an average paleotemperature of 21.8°C. This result shows that the carbonate karst fillings have undergone the following dissolution and filling processes: surface exposure, followed by shallow burial, and finally deep burial.

Discussion

Analysis of filling environments and paleokarst developmental periods

The $\delta^{18}O$ values of limestones and calcite paleokarst fillings from the Tazhong region show a bias towards negative values, and a large range of $\delta^{13}C$ values. This is related to the uplifting of the surface during the Ordovician period, which placed the entire surface in an open environment, thus causing widespread dissolution by atmospheric precipitation, whose CO_3^{2-} anions are characteristically highly enriched in ^{12}C and ^{16}O (Gasparrini et al., 2006; Azmy et al., 2009).

Based on the $\delta^{13}C$-$\delta^{18}O$ relational diagram shown in Figure 5, the calcite Ordovician carbonate paleokarst fillings can be divided based on their paleokarst depositional environments into 4 different types, as shown in Table 2.

Type I is a marine depositional environment that reflects the isotopic characteristics of the syndiagenetic marine depositional environment as well as early paleokarstification and sedimentation. The calcite fillings within the karst fractures and cavities of Ordovician Yingshan Formation carbonates have $\delta^{13}C$ values of 1.77–2.48% and $\delta^{18}O$ values of −7.26 to -3.97%. The burial depth, temperature, and leaching dissolution of the sediments have an effect on $\delta^{13}C$ and $\delta^{18}O$ value. As the salinity increases, the $\delta^{13}C$ and $\delta^{18}O$ values both increase. The $\delta^{18}O$ value decreases as temperature increases; as the temperature and burial depth increase, the $\delta^{18}O$ value will become biased towards negative values (McCaig et al., 2000). As the $\delta^{13}C$ value is intimately related to paleosalinity, and is only weakly affected by temperature, its value closely reflects the depositional environment of these syndiagenetic marine paleokarsts.

Type II is an atmospheric freshwater karstification environment, which reflects on the isotopic characteristics of the atmospheric freshwater karstification and depositional environment that occurred during the period in which bare

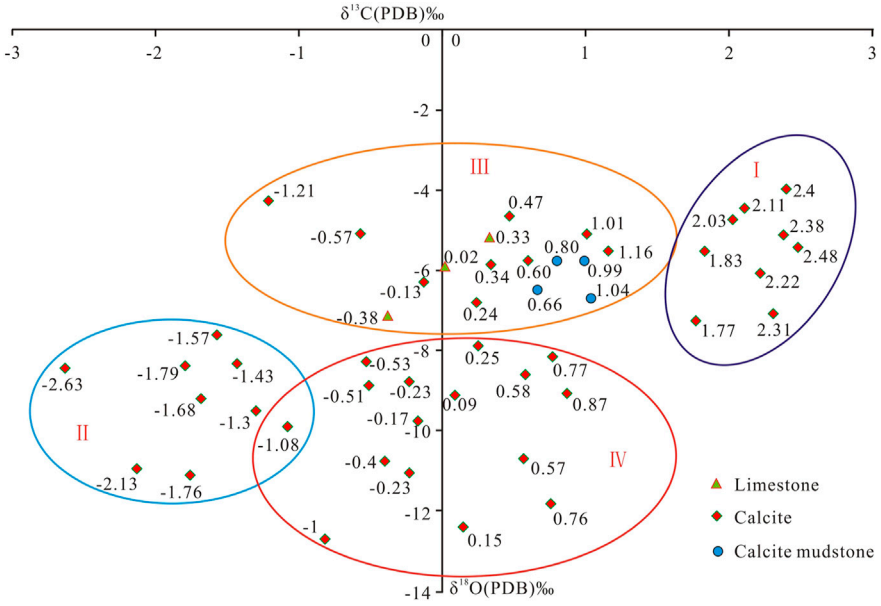

FIGURE 5
Bivariate δ13C-δ18O plot of Ordovician paleokarst fissure filings from the Tazhong region. Roman numerals refer to developmental periods shown in Table 2.

TABLE 2 Paleokarst developmental periods and characteristics of corresponding filling environment.

Developmental period	Formative environment	Isotopic characteristics	
		$\delta^{13}C$(PDB)‰	$\delta^{18}O$(PDB)‰
I	Marine deposition and filling	1.77~2.48	−7.26~-3.97
II	Atmospheric freshwater karstification	−2.63~−1.08	−11.11~−7.61
III	Shallow burial karstification	−1.21~1.16	−9.11~−4.62
IV	Deep burial karstification	−1.01~0.76	−12.70~−9.77

paleokarsts were exposed *via* the weathering crust. The calcite paleokarst fissure fillings had $\delta^{13}C$ values in the range of −2.63 to −1.08%, and $\delta^{18}O$ values in the range of −11.11 to -7.61%. Due to the influence of atmospheric freshwater (Gasparrini et al., 2006), the $\delta^{13}C$ value of the fillings is significantly lower than that of the bedrock, as these were formed in an open to semi-open environment. Atmospheric precipitation infiltrates along fractures and joints, dissolving and filling the carbonate bedrock to form fractures and cavities. As the diagenetic $\delta^{18}O$ value is determined by the temperature and isotopic composition of the medium, and atmospheric freshwater is depleted in ^{18}O but enriched in ^{12}C, $\delta^{13}C$ drifts towards negative values, while $\delta^{18}O$ tends towards highly negative values (Shields et al., 2003).

Type III is a shallow-burial karstification environment, in which calcite karst fissure fillings have $\delta^{13}C$ values of −1.21 to 1.16% and $\delta^{18}O$ values of −9.11 to −4.62%. The $\delta^{18}O$ value is significantly biased towards negative values, while the $\delta^{13}C$ value spans both negative and positive values, which indicates that the paleokarsts have undergone freshwater karstification before entering the shallow-burial kastification period: i.e., a successive mode of paleokarst development. Furthermore, the decomposition and methanation (CH_4) of organic material by methanogenic bacteria creates ^{12}C-enriched CH_4 and ^{13}C-enriched CO_2. Since the CO_2 released from methane fermentation participates in paleokarstification and deposition processes, the calcite fillings in the karst fractures and cavities become enriched in ^{13}C. The 3 micritic limestone (bedrock) samples and 4 calcite mudstone cavity-filling

samples all have carbon-isotope ratios that fall within this range.

Type IV is a deep-burial karstification environment, whose calcites have $\delta^{13}C$ values of −1.01 to 0.76% and $\delta^{18}O$ values of −12.70 to −9.77%, thus showing more negative $\delta^{18}O$ values. This study's calculations show that the paleotemperatures reached a maximum of 47.1°C, indicating that hot fluids played a significant role in the Formation and burial conditions of these calcite karst fissure fillings. As the fillings were affected and altered by ^{18}O-deficient hot fluids from deep regions during the deep burial stage, its $\delta^{18}O$ values characteristically show a significant negative bias (Lavoie and Chi 2006; Liu et al., 2012).

Geological significance

Changes in the carbon and oxygen isotopic compositions of carbonates are an embodiment of changes in the paleoclimate and paleooceanic environment, and thus serve as useful aids for studies of geological processes and depositional characteristics (Loucks 1999). The karst developments of carbonate rocks of Ordovician Yingshan Formation in Tazhong area are filled to different degrees by calcite and calcite mudstones. Early calcite fillings show bead-like dissolution pores that are caused by dissolution in a later period, and thus reflect the multi-periodic characteristics of the paleokarst.

Under equilibrium isotope fractionation, $\delta^{18}O$ is mainly controlled by environmental temperature changes, and the temperature-controlled water-rock reactions and isotopic fractionation coefficient gives the $\delta^{18}O$ value a −0.24%/°C temperature gradient (Hendy and Wilson 1986). The $\delta^{18}O$ values of calcite and calcite mudstones in Tazhong paleokarst fillings tend towards negative values, far below that of seawater, thus showing that the karst was developed through the influence of atmospheric precipitation in paleoweathering crusts.

As the burial depth increases, temperature and pressure also increase. The $\delta^{13}C$ values do not change as prominently as $\delta^{18}O$ values and tend to be more stable, as they are primarily determined by the organic carbon content and hydrocarbon (CH_4) conversion within the rocks. However, as compared to $\delta^{18}O$, $\delta^{13}C$ is more easily affected by evaporation, kinetic fractionation and early deposition of carbonates, causing its value to become biased towards positive values (Gent et al., 2001; Guo et al., 2010).

The calcite and calcite mudstone fillings in this research area have $\delta^{13}C$ (PDB) values between 2.48% and −2.13%, with an average value of 0.23%. The $\delta^{13}C$ values span a larger range and tend towards both extremes, signifying the presence of mixed seawater-freshwater karstification. This also reveals that the karsts have undergone multiple periods of transformation, including syndiagenesis, freshwater karstification, and burial karstification.

Based on statistical analysis of the conventional physical properties of 252 rock cores drilled from 25 wells, the experimentally measured porosity was 0.16%–11.25%, with an average of 0.82%; the measured permeability was 0.005–161 mD, with an average of 3.667 mD; the permeability as interpreted from well logs ranged from 0.007 to 225.532 mD, with an average value of 2.895 mD. This indicates that the porosity of the Yingshan Formation matrix primarily consists of low-porosity and low-permeability reservoirs, and that the effective reservoirs are mainly fracture-cavity systems composed of dissolved fractures, pores and cavities formed by paleokarstification. This finding thus provides a direction for the exploration and development of oil and gas fields and the prediction of favorable reservoir zones in the Tazhong region within the Tarim basin. Urey, 1948, Kuypers et al., 1999, Liu et al., 2004, Li, 2022a, Li et al., 2019, Li et al., 2022, Li et al., 2022b, Zhang et al., 2022a, Zhang et al., 2022b, Zhang et al., 2022c, Zhang et al., 2022d, Fan et al., 2022.

Conclusion

Using typical calcite and calcite mudstone paleokarst fissure-filling samples that are representative of the region, the stable carbon and oxygen isotopic characteristics of these samples were analyzed, and the developmental periods and depositional environment of the paleokarsts were reconstructed. The analysis of calcite carbon and oxygen isotopic ratios indicated that their $\delta^{13}C$ (PDB) values spanned a relatively large range, from 2.48% to −2.13%, with an average value of 0.23%; its $\delta^{18}O$ values ranged from −3.97% to −12.7%, with an average value of −7.64%.

The paleotemperatures at which the fillings were deposited within the paleokarst fissures was found to range from 6.5°C to 47.1°C, with an average value of 21.8°C. The Z values of the medium salinity ranged between 117.48 and 130.24, with an average value of 123.94; $\delta^{13}C$ values were found to correlate closely with the Z value, with a correlation coefficient of 0.958. Four types of carbonate paleokarstification and depositional environments have thus been revealed: a marine syndiagenetic depositional environment, an atmospheric freshwater karst-filling environment, a shallow-burial karstification paleoenvironment, and a deep-burial, high-temperature paleoenvironment. These results show that the dissolved pores, cavities and fractures formed by paleokarstification during later periods are the main effective reservoir spaces within the Tazhong region, thus providing a scientific basis for well placements in exploration and development work, and karst reservoir predictions.

Data availability statement

The original contributions presented in the study are included in the article/supplementary material, further inquiries can be directed to the corresponding author.

Author contributions

All authors listed have made a substantial, direct, and intellectual contribution to the work and approved it for publication.

Acknowledgments

We would like to thank the National Key Research and Development Program (No. 2018YFC0604301), the National Natural Science Foundation of China (No. 41302122), the Geological Survey Program of the China Geological Survey (No. DD20190562 and DD20221658), and the basic research program of Institute of Karst Geology, Chinese Academy of Geological Sciences (No. 2021008) for supporting this article. We would also like to express our sincere gratitude to the reviewers and editors for their valuable comments on this article.

Conflict of interest

The authors declare that the research was conducted in the absence of any commercial or financial relationships that could be construed as a potential conflict of interest.

Publisher's note

All claims expressed in this article are solely those of the authors and do not necessarily represent those of their affiliated organizations, or those of the publisher, the editors and the reviewers. Any product that may be evaluated in this article, or claim that may be made by its manufacturer, is not guaranteed or endorsed by the publisher.

References

Arthur, M. A., Dean, W. E., and Pratt, L. M. (1988). Geochemical and climatic effects of increased marine organic carbon burial at the Cenomanian/Turonian boundary. *Nature* 335, 714–717. doi:10.1038/335714a0

Azmy, K., Knight, I., Lavoie, D., and Chi, G. (2009). Origin of dolomites in the boat harbour formation, st. George group, in Western newfoundland, Canada: Implications for porosity development. *Bull. Can. Petroleum Geol.* 57 (1), 81–104. doi:10.2113/gscpgbull.57.1.81

Chen, J. S., Li, Z., Wang, Z. Y., Tan, X. C., Li, L., and Ma, Q. (2007). Paleokarstification and reservoir distribution of ordovician carbonates in Tarim basin. *Acta Sedimentol. Sin.* 25 (6), 858–868. (in Chinese).

Craig, H. (1961). Isotopic variations in meteoric waters. *Science* 133, 1702–1703. doi:10.1126/science.133.3465.1702

Epstein, S., and Mayeda, T. K. (1953). Variation of O18 content of waters from natural sources. *Geochim. Cosmochim. Acta* 4, 213–224. doi:10.1016/0016-7037(53)90051-9

Fan, C. H., Xie, H. B., Li, H., Zhao, S. X., Shi, X. C., Liu, J. F., et al. (2022). Complicated fault characterization and its influence on shale gas preservation in the southern margin of the Sichuan Basin, China. *Lithosphere*, 8035106. doi:10.2113/2022/8035106

Gao, Q. D., Zhao, K. Z., Hu, X. F., and Pan, W. Q. (2011). C-O, Sr isotope composition of the carbonate in Ordovician in Tarim Basin and implication for fluid origin. *J. Zhejiang Univ. Sci. Ed.* 38 (5), 579–583. (in Chinese).

Gasparrini, M., Bechstaedt, T., and Boni, M. (2006). Massive hydrothermal dolomites in the southwestern Cantabrian Zone (Spain) and their relation to the Late Variscan evolution. *Mar. Pet. Geol.* 23 (5), 543–568. doi:10.1016/j.marpetgeo.2006.05.003

Gent, D. D., Baker, A., Massault, M., Proctor, C., Gilmour, M., Pons-Branchu, E., et al. (2001). Dead carbon in stalagmites: Carbonate bedrock paleodissolution vs. ageing of soil organic matter: Implications for ^{13}C variations in speleothems. *Geochim. Cosmochim. Acta* 20, 3443–3457. doi:10.1016/s0016-7037(01)00697-4

Gu, J. Y. (2000). Characteristics and origin analysis of dolomite in lower Ordovician of Tarim Basin. *XJ Pet. Geol.* 21 (2), 120–122. (in Chinese).

Guo, H., Du, Y. S., and Huang, J. H. (2010). Habitat types and palaeoenvironments of the mesoproterozoic gaoyuzhuang Formation in pingquan, hebei province. *J. Palaeogeogr.* 12 (3), 269–280.

Han, J. F., Zhang, H, Z., Yu, H. F., Ji, Y. G., Sun, C. H., Han, J., et al. (2012). Hydrocarbon accumulation characteristics and exploration on large marine carbonate condensate field in Tazhong Uplift. *Acta Petrol. Sin.* 28 (3), 769–782. (in Chinese).

Hendy, C. H., and Wilson, A. T. (1986). Palaeoclimatic data from speleothems. *Nature* 216, 48–51. doi:10.1038/219048a0

Huang, S. J., Lan, Y. F., Huang, K. K., and Lu, J. (2014). Vug fillings and records of hydrothermal activity in the middle permian qixia formation,Western sichuan basin. *Acta Petrol. Sin.* 30 (3), 687–698. (in Chinese).

Huang, S. J., Li, X. N., Hu, Z. W., Liu, S. B., Huang, K. K., and Zhong, Y. J. (2016). Comparison of carbon and oxygen isotopic composition of Feixianguan carbonates, Early Triassic, between east and west sides of Kaijiang-Liangping trough, Sichuan Basin, and the significance for paleoceanography. *Geochimica* 45 (1), 24–40. (in Chinese).

Keith, M. H., and Weber, J. N. (1964). Carbon and oxygen isotopic composition of selected limestones and fossils. *Geochim. Cosmochim. Acta* 28 (11), 1787–1816. doi:10.1016/0016-7037(64)90022-5

Kuypers, M. M., Pancost, R. D., and Sinninghe Damsté, J. S. (1999). A large and abrupt fall in atmospheric CO_2 concentration during Cretaceous times. *Nature* 399, 342–345. doi:10.1038/20659

Lavoie, D., and Chi, G. X. (2006). Hydrothermal dolomitization in the lower silurian La vieille Formation in northern new brunswick: Geological context and significance for hydrocarbon exploration. *Bull. Can. Petroleum Geol.* 54 (4), 380–395. doi:10.2113/gscpgbull.54.4.380

Li, D., Liang, D., and Jia, C. (1996). Hydrocarbons accumulations in the Tarim basin, China. *AAPG Bull.* 80, 1587–1603.

Li, H. (2022a). Research progress on evaluation methods and factors influencing shale brittleness: A review. *Energy Rep.* 8, 4344–4358. doi:10.1016/j.egyr.2022.03.120

Li, H., Tang, H. M., Qin, Q. R., Zhou, J. L., Qin, Z. J., Fan, C. H., et al. (2019). Characteristics, formation periods and genetic mechanisms of tectonic fractures in the tight gas sandstones reservoir: A case study of xujiahe Formation in YB area, sichuan basin, China. *J. Pet. Sci. Eng.* 178, 723–735. doi:10.1016/j.petrol.2019.04.007

Li, H., Zhou, J. L., Mou, X. Y., Guo, H. X., Wang, X. X., An, H. Y., et al. (2022b). Pore structure and fractal characteristics of the marine shale of the longmaxi Formation in the changning area, southern sichuan basin, China. *Front. Earth Sci.* 10, 1018274. doi:10.3389/feart.2022.1018274

Li, J., Li, H., Yang, C., Wu, Y. J., Gao, Z., and Jiang, S. L. (2022). Geological characteristics and controlling factors of deep shale gas enrichment of the Wufeng-Longmaxi Formation in the southern Sichuan Basin, China. *Lithosphere*, 4737801. doi:10.2113/1970/4737801

Li, X. Q., and Wan, G. J. (1999). Problems in studies on carbon and oxygen stable isotopes in carbonates. *Adv. Earth Sci.* 14 (3), 262–268.

Liu, C. G., Li, G. R., Zhu, C. L., and Liu, G. Y. (2008). Geochemistry characteristics of carbon, oxygen and strontium isotopes of calcites filled in karstic fissure-cave in lower-middle Ordovician of Tahe Oilfield, Tarim Basin. *Earth Science-Journal China Univ. Geosciences* 33 (3), 377–386. (in Chinese).

Liu, J. Q., Li, Z., Huang, J. C., and Yang, L. (2012). Distinct sedimentary environments and their influences on carbonate reservoir evolution of the Lianglitag Formation in the Tarim basin, Northwest China. *Sci. China Earth Sci.* 42 (12), 1641–1655. doi:10.1007/s11430-012-4457-5

Liu, K. Y., Bourdet, J., Zhang, B. S., Zhang, N., Lu, X., Liu, S., et al. (2013). Hydrocarbon charge history of the Tazhong Ordovician reservoirs, Tarim

Basin as revealed from an integrated fluid inclusion study. *Petroleum Explor. Dev.* 40 (2), 183–193. (In Chinese). doi:10.1016/s1876-3804(13)60021-x

Liu, X. P., Wu, X. S., and Zhang, X. Z. (2004). Geochemistry characteristics of carbon and oxygen isotopes of Ordovician carbonate paleokarst reservoir in the Western region of Lungu, Tarim Basin. *J. Xi'an Shiyou Univ. Nat. Sci. Ed.* 19 (4), 69–72. (in Chinese).

Liu, Z. H., Dai, Y. N., and Lin, Y. S. (2004). Paleoenvironmental reconstruction based on hydrochemistry and tufa stable isotopes: Case study of Xiangshui River, LiBo, Guizhou. *Quatern Sci.* 24 (4), 447–454. (in Chinese).

Liu, Z. H., Yuan, D. X., and He, S. Y. (1997). Stable carbon isotope geochemical and hydrochemical features in the system of carbonate-H_2O-CO_2 and their implications: Evidence from several typical karst areas of China. *Acta Geol. Sin.* 71 (3), 281–288. (in Chinese).

Loucks, R. G. (1999). Paleocave carbonate reservoirs: Origins, burial-depth modification, spatial complexity, and reservoir implications. *AAPG Bull.* 83 (11), 1795–1834.

Lu, H. Z., and Shan, Q. (2015). Composition of ore forming fluids in metal deposits and fluid inclusion. *Acta Petrol. Sin.* 31 (4), 1108–1116. (in Chinese).

Luo, C. S., Yang, H. J., Li, J. H., Xie, H. W., and Huang, G. J. (2011). Characteristics of high quality Ordovician reservoirs and controlling effects of faults in the Tazhong area, Tarim Basin. *Petroleum Explor. Dev.* 38 (6), 716–724. (in Chinese).

McCaig, A. M., Tritlla, J., and Banks, D. A. (2000). Fluid mixing and recycling during Pyrenean thrusting: Evidence from fluid inclusion halogen ratios. *Geochim. Cosmochim. Acta* 64, 3395–3412. doi:10.1016/s0016-7037(00)00437-3

Scholle, P. A., and Arthur, M. A. (1980). Carbon isotope fluctuations in Cretaceous pelagic limestones: Potential stratigraphic and petroleum exploration tool. *AAPG Bull.* 64, 67–87.

Shao, Y. L. (1994). The relation of the oxygen and carbon isotope in the carbonate rocks to the paleotemperature etc. *J. China Univ. Min. Technol.* 23 (1), 39–45. (in Chinese).

Shen, A. J., Wang, Z. M., Yang, H. J., and Ni, X. F. (2006). Genesis classification and characteristics of Ordovician carbonate reservoirs and petroleum exploration potential in Tazhong region, Tarim basin. *Mar. Orig. Pet. Geol.* 11 (4), 1–12. (in Chinese).

Shields, G. A., Carden, G. A., Veizer, J., Meidla, T., Rong, J. Y., and Li, R. Y. (2003). Sr, C and O isotope geochemistry of ordovician brachiopods: A major isotopic event around the middle-late ordovician transition. *Geochim. Cosmochim. Acta* 67 (11), 2005–2025. doi:10.1016/s0016-7037(02)01116-x

Sun, C. H., Yu, H. F., Wang, H. S., Liu, H., Zhang, Z. H., Han, J., et al. (2012). Vugular formation of carbonates in Ordovician Yingshan reservoir in Tazhong northern slope of Tarim basin. *Nat. Gas. Geosci.* 23 (2), 230–236. (in Chinese).

Taylor, H. P. (1968). The oxygen isotope geochemistry of igneous rocks. *Contr. Mineral. Petrol.* 19, 1–71. doi:10.1007/bf00371729

Tian, J. C., and Zheng, Y. F. (1995). The evolution pattern of the carbon and oxygen isotopes in the Permian marine carbonate rocks from Guizhou. *J. Chengdu Inst. Technol.* 22 (1), 78–82. (in Chinese).

Urey, H. C. (1948). Oxygen isotopes in nature and in the laboratory. *Science* 108, 489–496. doi:10.1126/science.108.2810.489

Valley, J. W., and Cole, D. R. (2001). Stable isotope geochemistry. *Rev. Mineral. Geochem* 43, 1–662.

Wang, B. Q., and Al-Aasm, I. S. (2002). Karst-controlled diagenesis and reservoir development: Example from the Ordovician main-reservoir carbonate rocks. *AAPG Bull.* 86 (9), 1639–1658.

Wang, Q., Wang, X. Z., Xu, J. L., and Liu, Z. K. (2014). Carbon and oxygen isotope stratigraphy research in Chashgui area. *J. Southwest Petroleum Univ. Sci. Technol. Ed.* 36 (3), 27–34. (in Chinese).

Wu, G. H., Li, H. H., Zhang, L. P., Wang, C. L., and Zhou, B. (2012). Reservoir forming conditions of the Ordovician weathering crust in the Maigaitislope, Tarim basin, NW China. *Petroleum Explor. Dev.* 39 (2), 144–153. (in Chinese).

Yang, H. J., Li, K. K., Pan, W. Q., Xiao, Z. Y., and Cai, C. F. (2012). Burial hydrothermal dissolution fluid activity and its transforming effect on the reservoirs in Ordovician in Central Tarim. *Acta Petrol. Sin.* 28 (3), 783–792. (in Chinese).

Zhang, B., Zheng, R. C., Wang, X. B., Luo, Y., Li, W., Wen, H. G., et al. (2011). Paleokarst features and reservoir distribution in the Huanglong Formation of eastern Sichuan. *Petroleum Explor. Dev.* 38 (3), 257–267. (in Chinese). doi:10.1016/s1876-3804(11)60032-3

Zhang, K., Jiang, Z., Song, Y., Jia, C., Yuan, X., Wang, X., et al. (2022a). Quantitative characterization for pore connectivity, pore wettability, and shale oil mobility of terrestrial shale with different lithofacies -- A case study of the Jurassic Lianggaoshan Formation in the Southeast Sichuan Basin of the Upper Yangtze Region in Southern China. *Front. Earth Sci. (Lausanne).* 10, 864189. doi:10.3389/feart.2022.864189

Zhang, K., Song, Y., Jia, C., Jiang, Z., Han, F., Wang, P., et al. (2022b). Formation mechanism of the sealing capacity of the roof and floor strata of marine organic-rich shale and shale itself, and its influence on the characteristics of shale gas and organic matter pore development. *Mar. Petroleum Geol.* 140, 105647. doi:10.1016/j.marpetgeo.2022.105647

Zhang, K., Song, Y., Jiang, Z., Xu, D., Li, L., Yuan, X., et al. (2022d). Quantitative comparison of Genesis and pore structure characteristics of siliceous minerals in marine shale with different TOC contents - a case study on the shale of Lower Silurian Longmaxi Formation in Sichuan Basin, Southern China. *Front. Earth Sci. (Lausanne).* 10, 887160. doi:10.3389/feart.2022.864279

Zhang, K., Song, Y., Jiang, Z., Yuan, X., Wang, X., Han, F., et al. (2022c). Research on the occurrence state of methane molecules in post-mature marine shales-A case analysis of the Lower Silurian Longmaxi Formation shales of the upper Yangtze region in Southern China. *Front. Earth Sci. (Lausanne).* 10, 864279. doi:10.3389/feart.2022.887160

Zhang, Q. Y., Chen, L. X., Liang, B., Cao, J. W., Dan, Y., and Li, J. R. (2015). Research of geochemistry characteristics of carbon and oxygen isotopes of ordovician palaeokarst reservoir in the east of lungu-7, north Tarim basin. *Geol. Sci. Technol. Inf.* 34 (2), 52–56. (in Chinese).

Zhang, Q. Y., Liang, B., Qin, F. R., Cao, J. W., Dan, Y., and Li, J. R. (2016a). Environmental and geochemical significance of carbon and oxygen isotopes of Ordovician carbonate paleokarst in Lunnan, Tarim Basin. *Environ. Earth Sci.* 75 (14), 1074–1083. doi:10.1007/s12665-016-5882-0

Zhang, Q. Y., Qin, F. R., Liang, B., Cao, J. W., Dan, Y., Li, J. R., et al. (2016b). Characteristics of Ordovician paleokarst inclusions and their implications for paleoenvironmental and geological history in Halahatang area of northern Tarim Basin. *Carbonates Evaporites* 33, 43–54. doi:10.1007/s13146-016-0325-2

Zhang, X. L. (1985). Relationship between carbon and oxygen stable isotope in carbonate rocks and paleosalinity and paleotemperature of sea water. *Acta Sedimentol. Sin.* 3 (4), 17–30. (in Chinese).

Zhao, W. F., Liu, H. G., and Wang, G. L. (2012). C and O isotope geochemical characteristics of reservoir crevice fillings in Ordovician, Yuqi West Area. *J. Guizhou Univ. Nat. Sci.* 29 (3), 34–39. (in Chinese).

Zheng, Y. F., and Chen, J. F. (2000). *Stable isotope geochemistry*, 10. Beijing: Science Press, 12.

Zhong, J. H., Mao, C., Li, Y., Yuan, X., Niu, Y., et al. (2012). Discovery of the ancient ordovician oil-bearing karst cave in liuhuanggou, north Tarim basin and its significance. *Sci. China Earth Sci.* 55, 1406–1426. (in Chinese). doi:10.1007/s11430-012-4467-3

Zhu, G. Y., Zhang, S. C., Liang, Y. B., Dai, J., and Li, J. (2005). Isotopic evidence of TSR origin for natural gas bearing high H_2S contents within the Feixianguan Formation of the northeastern Sichuan Basin, southwestern China. *Sci. China Ser. D-Earth. Sci.* 48 (11), 1960–1971. (in Chinese). doi:10.1360/082004-147